http://dx.doi.org/10.7567/JJAP.52.011801

Investigation of Silicon Surface Passivation by Microwave Annealing Using Multiple-Wavelength Light-Induced Carrier Lifetime Measurement

Toshiyuki Sameshima*, Ryoko Ebina, Koichi Betsuin, Yuta Takiguchi, and Masahiko Hasumi

Tokyo University of Agriculture and Technology, Koganei, Tokyo 184-8588, Japan
E-mail: tsamesim@cc.tuat.ac.jp

Received September 2, 2012; revised October 19, 2012; accepted October 27, 2012; published online December 20, 2012

A simple annealing method using a commercial 2.45 GHz microwave oven is reported to increase the minority carrier lifetime τ_{eff} for 4-in.-size 500-μm-thick 20 Ω cm n-type silicon substrates coated with 100-nm-thermally grown SiO_2 layers. The microwave annealing was conducted with 2-mm-thick glass substrates, which sandwiched a silicon sample to maintain the thermal energy in silicon and realize gradual cooling. A 9.35 GHz microwave transmittance measurement system was used to measure τ_{eff} in the cases of continuous-wave 635 and 980 nm laser diode (LD) light illuminations. Radio-frequency Ar plasma irradiation at 50 W for 60 s to the top surface of a silicon sample markedly decreased τ_{eff} in the range from 6.0×10^{-6} to 2.4×10^{-5} s and from 4.2×10^{-5} to 6.4×10^{-5} s in the cases of 635 and 980 nm light illuminations, respectively, while τ_{eff} had the same distribution from 1.6×10^{-3} to 3.1×10^{-3} s for the initial samples. The finite element numerical analysis revealed that Ar plasma irradiation caused high densities of recombination defect states at the silicon top surface in the range from 1.3×10^{13} to 5.0×10^{13} cm^{-2}. Microwave annealing at 700 W for 120 s markedly increased τ_{eff} in the range from 8.0×10^{-4} to 2.5×10^{-3} s, which were close to those of the initial samples. The density of recombination defect states was well decreased by microwave annealing to low values in the range from 7.0×10^{10} to 3.4×10^{11} cm^{-2}. The high τ_{eff} achieved by microwave annealing was maintained for a long time above 5000 h.
© 2013 The Japan Society of Applied Physics

1. Introduction

The long minority carrier effective lifetime τ_{eff} of semiconductors is important for solar cells and photosensors.[1–11] A long τ_{eff} allows the minority carriers to well diffuse in the whole region of a semiconductor substrate with a low annihilation rate. It therefore results in a high short-circuit current-and a high open circuit voltage for semiconductor solar cells. It also gives high photo-sensitivity for photosensor devices. The amount of defect states causing carrier recombination should be reduced for achieving a long τ_{eff}. Surface passivation and improvement in the crystalline quality of semiconductors are therefore important. Several techniques have been developed for surface passivation, for example, hydrogenation[12,13] and high pressure H_2O vapor heat treatments.[14,15] Thermal annealing is also important to reduce the amount of defects generated during device fabrication processes. We have recently reported a marked decrease in τ_{eff} by plasma treatment, which is a very conventional method for semiconductor device fabrication processing.[16] Post-annealing is necessary to increase τ_{eff} again. Moreover, a short annealing in a low-temperature atmosphere is attractive in the low thermal budget for a low fabrication cost.

In this paper, we report the precise investigation of the change in τ_{eff} for n-type silicon substrates by a simple annealing method using a commercial 2.45 GHz microwave oven with no previous substrate heating.[17] We apply the present method to the curing of serious carrier recombination defects caused by Ar plasma irradiation. To investigate the change in τ_{eff}, we developed a system of microwave absorption induced by light illumination at wavelengths of 635 and 980 nm.[18–20] The penetration depth at 635 nm was about 3 μm, while it is very deep, 125 μm, for 980 nm light.[21] Photo-induced carriers generated in the deep region of semiconductors are alive until they meet carrier recombination defect states when a high density of carrier recombination defect states are localized at the surfaces. Therefore, τ_{eff} is high when carrier generation occurs in the deep region far from the surface. On the other hand, τ_{eff} is low when carrier generation occurs close to the carrier recombination defect states. In contrast, τ_{eff} will not depend on the carrier generation position if the density of carrier recombination defect states is low because a low recombination velocity allows a long carrier diffusion length longer than the substrate thickness. We report the τ_{eff} spatial distribution measured by light illumination with the two different wavelengths in the process steps of initial, Ar plasma, and microwave annealing treatments. We discuss carrier recombination velocity and recombination defect states on the basis of numerical analysis of the experimental results of τ_{eff}. We demonstrate that high τ_{eff} and low recombination defect density are achieved by microwave annealing. We also report that the high τ_{eff} is maintained for a long time.

2. Experimental Procedure

20 Ω cm n-type silicon substrates with a thickness of 500 μm and a diameter of 4 in. were prepared. The top and rear surfaces were coated with 100-nm-thick thermally grown SiO_2 layers. The top surfaces of the samples were irradiated by 13.56 MHz radio-frequency (RF) Ar plasma at 50 W and 1.0 Pa for 60 s, as shown by the schematic image in Fig. 1.[16] A sample was placed on a metal plate electrically grounded in a chamber facing a metal electrode. Ar gas was introduced at 5 sccm under evacuation using a turbo-molecular pump. Ar plasma was generated by applying RF voltage at the electrode at room temperature. Samples were subsequently treated with microwave irradiation using a commercial 2.45 GHz microwave oven at 700 W, as shown by the schematic image in Fig. 2. A silicon sample was sandwiched in two 2-mm-thick glass substrates with the low heat conductivity to keep heated energy in the silicon sample, as shown by cross section in Fig. 2. We also heated Ar plasma irradiated-sample at 500 °C using a furnace in comparison.

Figure 3 shows a schematic of the 9.35 GHz microwave transmittance measurement system with waveguide tubes, which had a narrow gap for placing a sample wafer. The X–Y moving stage moved the sample to measure the τ_{eff}

 © 2013 The Japan Society of Applied Physics

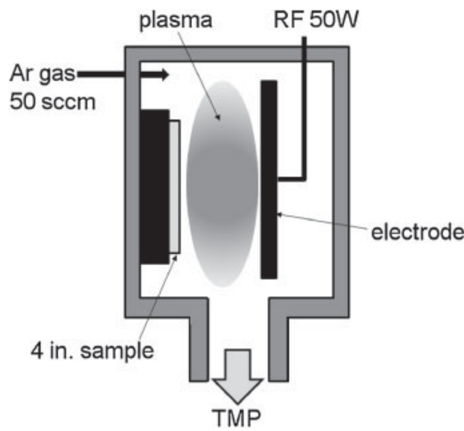

Fig. 1. Schematic of apparatus for 13.56 MHz RF Ar plasma irradiation at 50 W and at room temperature.

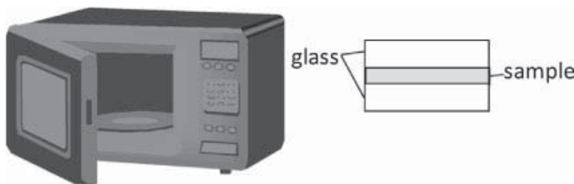

Fig. 2. Schematic of apparatus for microwave oven and sample treatment condition, in which a silicon sample was sandwiched by glass substrates.

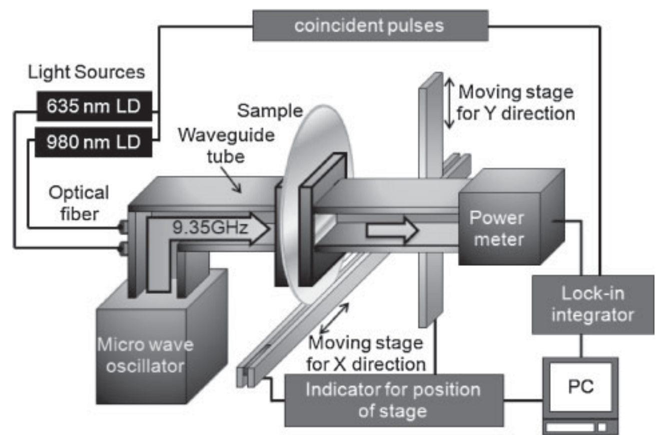

Fig. 3. Schematic of apparatus for a 9.35 GHz microwave transmittance measurement system for measuring τ_{eff} of sample wafers with 635 and 980 nm light illuminations.

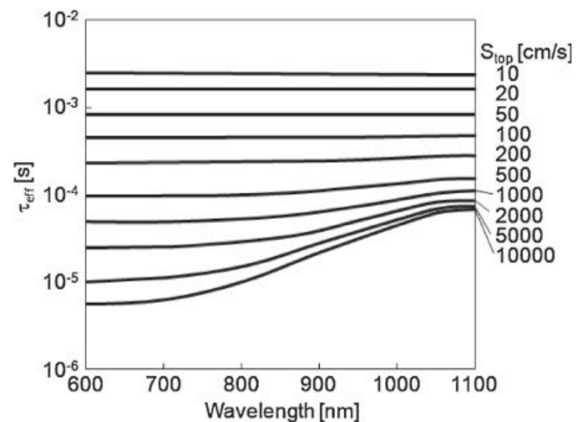

Fig. 4. Calculated τ_{eff} as a function of wavelength of light illuminated to the top surface under conditions of 20 Ω cm n-type 500-μm-thick silicon substrate with τ_b of 0.1 s, S_{rear} of 10 cm/s, and different S_{top} values ranging from 10 to 10000 cm/s.

spatial distribution over the whole surface area. Continuous wave (CW) 635 and 980 nm laser diode (LD) lights were introduced in the waveguide tube, as shown in Fig. 3. The light intensities were set at 1.5 and 0.98 mW/cm^2 at the sample surface for 635 and 980 nm lights, respectively, to realize the same photon flux between the two-different wavelength lights. The microwave which transmitted samples was rectified using a high-speed diode and was integrated. The integrated voltage was detected by a digital electrometer and analyzed to obtain τ_{eff}.[18–20] We constructed a finite-element numerical calculation program including theories of carrier generation associated with optical absorption coefficients,[21] carrier diffusion, and annihilation[18,19,22] for estimating the surface recombination velocity at the top surface S_{top} and the rear surface S_{rear} and the bulk lifetime τ_b. The most possible S_{top} and S_{rear} were determined by best coincidence between experimental and calculated τ_{eff}.

Figure 4 shows demonstration of the calculation of τ_{eff} as a function of the wavelength of the light illuminated to the top surface under the conditions of a 20 Ω cm n-type 500-μm-thick silicon substrate with a high τ_b of 0.1 s, S_{rear} of 10 cm/s, and different S_{top} values ranging from 10 to 10000 cm/s. When S_{top} was smaller than 50 cm/s, τ_{eff} was high and independent of the wavelength of the light. A small S_{top} results in a low annihilation probability of minority carriers and allows their diffusion throughout the whole substrate in the depth direction. The minority carriers therefore had the same carrier concentration distribution in the depth direction in the cases of different carrier generation depths. This is the reason why τ_{eff} was independent of the wavelength of the illuminating light. On the other hand, when S_{top} was 50 cm/s, τ_{eff} was small, 4.6×10^{-4} s, at 600 nm. It slightly increased as the wavelength increased and reached 5.0×10^{-4} s at 1100 nm. When S_{top} was large, minority carriers generated near the top surface by short-wavelength light illumination were rapidly annihilated by recombination defect states located at the top surface. In contrast, τ_{eff} was large in the case of long-wavelength light illumination because the low optical absorption coefficient at a long wavelength allowed minority carrier generation in deep regions. This effect became much more substantial as S_{top} increased. When S_{top} was 10000 cm/s, τ_{eff} was only 5.8×10^{-6} s at 600 nm. On the other hand, it was high, 7.1×10^{-5} s, at 1100 nm. τ_{eff} strongly depends on carrier generation depth in the case of a large surface recombination velocity.

3. Results and Discussion

The change in τ_{eff} with the duration of microwave irradiation was first investigated. Figure 5(a) shows τ_{eff} as a function of duration of 2.45 GHz microwave irradiation at 700 W for 120 s in the case of 635 nm light illumination for samples Ar plasma irradiated for 60 s. τ_{eff} was markedly decreased from 2.1×10^{-3} s (initial) presented by an arrow in Fig. 5 to

 © 2013 The Japan Society of Applied Physics

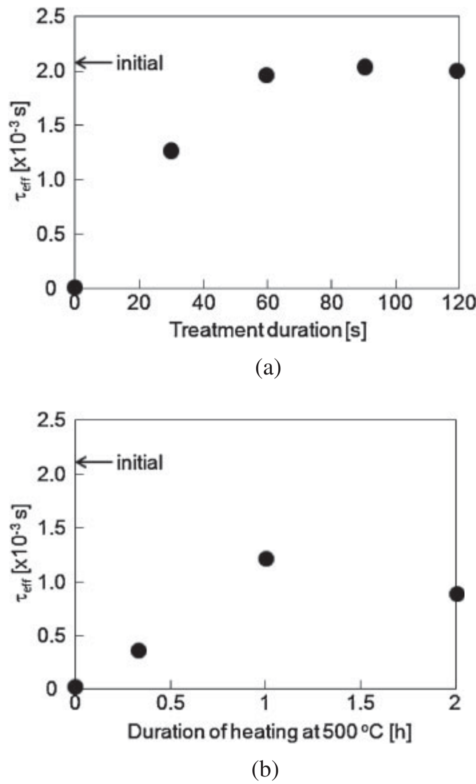

Fig. 5. τ_{eff} as a function of duration of 2.45 GHz microwave irradiation at 700 W for 120 s in the cases of 635 nm light illumination for samples Ar plasma irradiated for 60 s (a) and τ_{eff} as a function of duration of heating in the furnace at 500 °C for samples Ar plasma irradiated for 60 s (b). Arrows indicate τ_{eff} for the initial samples. Ar plasma irradiation decreased τ_{eff} to 1.9×10^{-5} s in the case of (a) and 2.0×10^{-5} s in the case of (b).

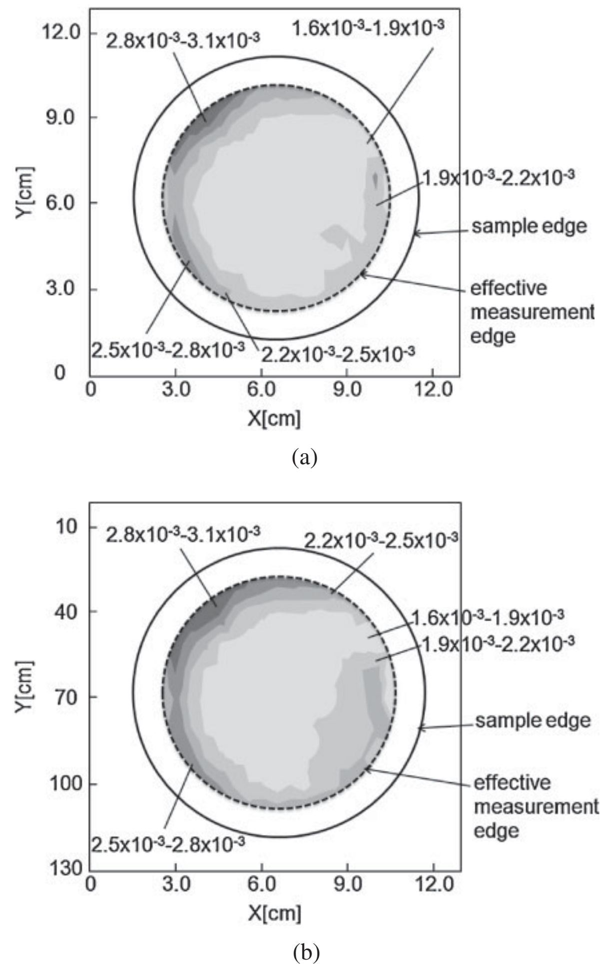

Fig. 6. τ_{eff} spatial distribution for the initial sample coated with 100-nm-thick thermally grown SiO_2 layers in the cases of 635 nm light illumination (a) and 980 nm light illumination (b). τ_{eff} in regions 1.2 cm from edges was not presented because our microwave tube had a cross of $2.3 \times 1.0\,cm^2$.

1.9×10^{-5} s by Ar plasma irradiation. τ_{eff} markedly increased to 2.0×10^{-3} s as the duration of microwave irradiation at 700 W increased to 60 s. The τ_{eff} of 2.0×10^{-3} s was almost the same value as the initial one. τ_{eff} almost leveled off for the duration of microwave irradiation between 60 and 120 s. This result in Fig. 5(a) shows that substantial carrier recombination defect states were generated in the sample by Ar plasma irradiation for 60 s, so that τ_{eff} seriously decreased from the initial values. It also shows that the carrier recombination defect states were markedly decreased by microwave irradiation at 700 W for a short time. Figure 5(b) presents τ_{eff} as a function of duration of heating in the furnace at 500 °C for an Ar plasma-irradiated sample. τ_{eff} was decreased to 2.0×10^{-5} s by Ar plasma irradiation for 60 s. It was increased to 1.2×10^{-3} s by heating in the furnace as the heating duration increased to 1 h. It was much higher than that of the as-Ar plasma treated sample, but still lower than the initial value of 2.1×10^{-3} s. τ_{eff} almost leveled off for heating at 500 °C up to 2 h. Heat treatment at 500 °C for 1 h was effective in curing carrier recombination defect states caused by Ar plasma, but it was not sufficient to make the surface state return to the initial state. The present microwave irradiation effectively cured the carrier recombination defect sites with in a short time in room-temperature atmosphere, as shown in Fig. 5(a). On the basis of the result in Fig. 5, we set the duration of microwave irradiation to 120 s for the following measurements of the τ_{eff} spatial distribution. Figure 6 shows τ_{eff} spatial distribution for the initial 4-in.-size sample in the cases of 635 nm light illumination (a) and 980 nm light illumination (b). τ_{eff} in regions 1.2 cm from the sample edges was not presented because our microwave tube had a cross section of $2.3 \times 1.0\,cm^2$. Accurate measurement was not possible in the edge regions. τ_{eff} had high values in the range from 1.6×10^{-3} to 3.1×10^{-3} s in both the light illumination cases, as shown in Fig. 6. This means that the silicon surface was well passivated by the thermally grown SiO_2 layers. The calculation result in Fig. 4 supports that low S_{top} and S_{rear} resulted in the same τ_{eff} for the cases of 635 and 980 nm light illumination. Figure 7 shows the τ_{eff} spatial distribution for the sample Ar plasma irradiated for 60 s in the cases of 635 nm light illumination (a) and 980 nm light illumination (b). τ_{eff} markedly decreased to values in the range from 6.0×10^{-6} to 2.4×10^{-5} s in the case of 635 nm light illumination. On the other hand, τ_{eff} distributed from 4.2×10^{-5} to 6.4×10^{-5} s in the case of 980 nm light illumination, as shown in Fig. 7(b). The results in Fig. 7 show that substantial recombination defect states were generated by Ar plasma irradiation in the silicon surface region. Figure 8 shows the τ_{eff} spatial distribution for the sample subsequently treated with 2.45 GHz microwave irradiation at 700 W for 120 s in the cases of 635 nm light illumination (a) and 980 nm light

 © 2013 The Japan Society of Applied Physics

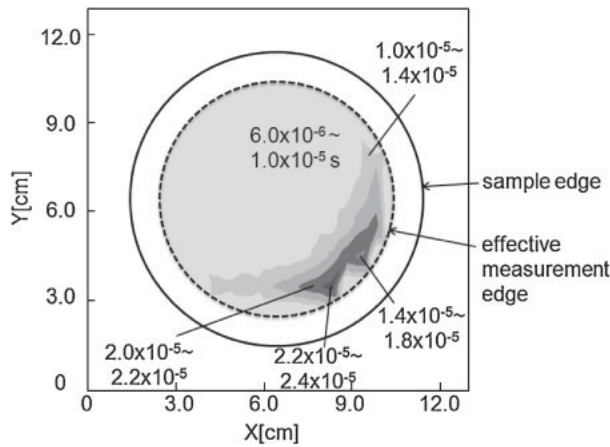

(a)

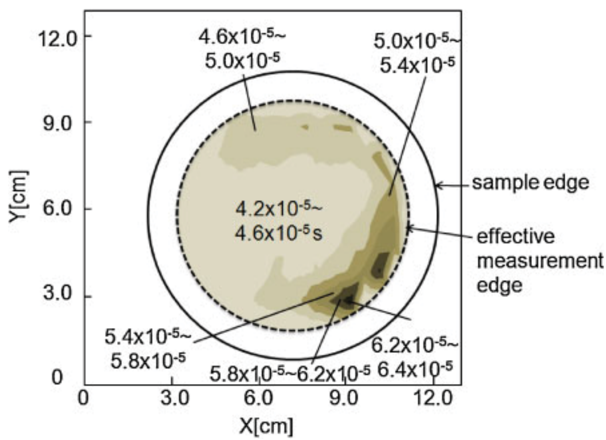

(b)

Fig. 7. (Color online) τ_{eff} spatial distribution for the sample Ar plasma irradiated for 60 s in the cases of 635 nm light illumination (a) and 980 nm light illumination (b).

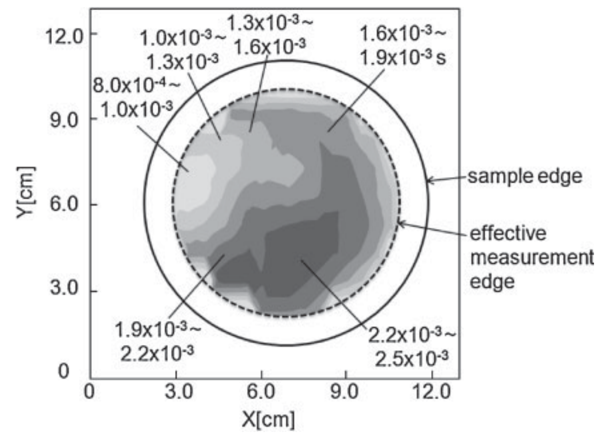

(a)

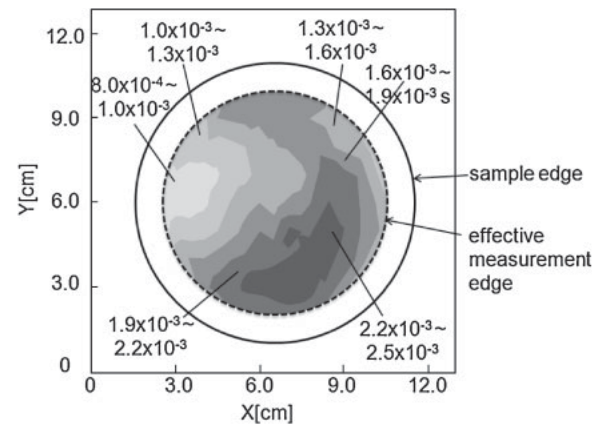

(b)

Fig. 8. τ_{eff} spatial distribution for the sample subsequently treated with 2.45 GHz microwave irradiation at 700 W for 120 s in the cases of 635 nm light illumination (a) and 980 nm light illumination (b).

illumination (b). τ_{eff} markedly increased to values in the range from 8.0×10^{-4} to 2.5×10^{-3} s in the case of 635 nm light illumination, and τ_{eff} had almost the same distribution in the case of 980 nm as that for 635 nm light illumination. Free majority electrons in silicon substrates absorbed the 2.45 GHz microwave and the substrates were effectively heated during operation of the microwave oven. Although the temperature increase was not precisely measured, our careful visual observation indicated that the samples were not heated higher than 700 °C for the 700 W microwave irradiation treatment for 120 s because the color of the samples was still very dark during microwave irradiation. The dark light emission from the sample was governed by the black body radiation rule. The substrate cooled down after termination of the microwave irradiation. The glass substrates that covered the both sides of silicon surface played the role of thermal insulators because of their low heat conductivity.[23] We believe that gradual cooling was achieved with a low cooling rate, which was essential for realizing a low density of defect states.[24]

Figure 9 shows the calculated relations (curves) of τ_{eff} in the cases of 635 nm (horizontal) and 980 nm (vertical) light illumination under the conditions of τ_b of 0.1 s, S_{rear} of 8 cm/s, and S_{top} ranging from 8 to 30000 cm/s. The calculated τ_{eff} had the same values between 635 and 980 nm illumination cases for τ_{eff} higher than 7.0×10^{-4} s. On the other hand, τ_{eff} for the 980 nm illumination case was larger than that for 635 nm illumination case when τ_{eff} was lower than 7.0×10^{-4} s. τ_{eff} decreased to 2.9×10^{-6} s as S_{top} increased to 30000 cm/s in the case of 635 nm light illumination, while it was still high at 3.9×10^{-5} s at an S_{top} of 30000 cm/s in the case of 980 nm light illumination because a diffusion time was necessary for carriers generated in the deep region by 980 nm light illumination to reach the top surface. Figure 9 also shows the experimental relations (dots) of τ_{eff} for the cases of 635 nm (horizontal) and 980 nm (vertical) light illumination for the initial (a), as-Ar plasma-irradiated (b), and subsequent microwave-annealed (c) samples. The experimental τ_{eff} for the initial sample had a good agreement with the calculated curves with S_{top} ranging from 8 to 23 cm/s. From the relations between the recombination velocity and the density of surface recombination defect states, which Fitzgerald and Grove reported,[25] the results in Fig. 9(a) show that the initial samples had a low density of surface recombination defect states in the range from 5.0×10^{10} to 1.5×10^{11} cm^{-2}. The τ_{eff} was markedly decreased by Ar plasma irradiation. The relations of τ_{eff} between 635 and 980 nm illumination agreed well with the calculated relation, as shown in Fig. 9(b). This clearly means

 © 2013 The Japan Society of Applied Physics

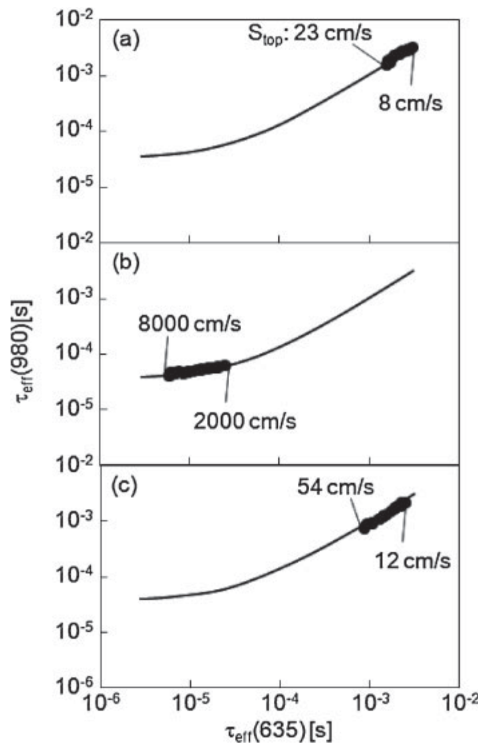

Fig. 9. Calculated relations of τ_{eff} for the cases of 635 nm (horizontal) and 980 nm (vertical) light illumination under the conditions of τ_b of 0.1 s, S_{rear} of 8 cm/s, and S_{top} ranging from 8 to 30000 cm/s. The figure also presents experimental relations of τ_{eff} for the cases of 635 nm (horizontal) and 980 nm (vertical) light illumination for initial (a), as-Ar plasma irradiated (b), and microwave-annealed (c) samples.

that Ar plasma irradiation caused substantial recombination defect states at the interface of SiO_2/Si. Deep ultra violet light generated from Ar plasma probably caused serious damage in silicon and resulted in serious recombination defect states. The result in Fig. 9(b) shows S_{top} ranging from 2000 to 8000 cm/s, which gives a density of recombination defect states ranging from 1.3×10^{13} to 5.0×10^{13} cm^{-2}. The wide distribution of the density of recombination defect states probably resulted from non-uniformity of the plasma density in our equipment. High surface recombination velocity means low photo sensitivity. This is a serious problem for photosensitive devices such as solar cells and photo sensors because plasma processing is widely used in semiconductor device fabrication.

Microwave irradiation treatment markedly increased τ_{eff} to close to those of the initial samples, as shown in Figs. 9(a) and 9(c). S_{top} decreased to values in the range from 12 to 54 cm/s. This indicated that the density of surface recombination defect states decreased to values in the range from 7.6×10^{10} to 3.4×10^{11} cm^{-2}. The density of recombination defect states caused by Ar plasma irradiation was effectively reduced by microwave irradiation. Similar τ_{eff} spatial distribution patterns were observed between the samples treated with Ar plasma irradiation and subsequent microwave annealing, as shown in Figs. 9(b) and 9(c). The regions in which Ar plasma irradiation decreased τ_{eff} to very low values still had a low τ_{eff} after microwave irradiation annealing. This indicates that an optimized condition to realize a high τ_{eff} everywhere has not yet been found.

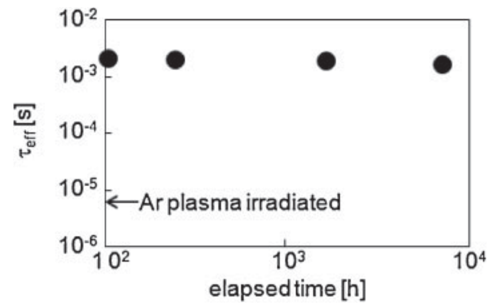

Fig. 10. τ_{eff} as a function of elapsed time after microwave annealing at 700 W for 120 s for samples treated with Ar plasma irradiation.

Moreover, we believe that the microwave intensity is not yet uniform in our commercial equipment. Conformation of the uniformity of microwave intensity and the design of a uniform microwave irradiation system are important for practical application to device fabrication.

Figure 10 shows τ_{eff} measured in a central region of the sample as a function of elapsed time after microwave annealing at 700 W for 120 s for samples treated with Ar plasma irradiation. τ_{eff} maintained high values for a long time, above 5000 h. This means that stable reduction of recombination defect states caused by Ar plasma irradiation was successfully achieved by microwave annealing.

The experimental results of Figs. 5 to 10 demonstrated the simple-thermal passivation method using microwave irradiation. Free carriers in silicon effectively absorbed the microwave and silicon samples were heated. The two glass substrates probably played the role of maintaining heat energy. Gradual cooling with a low cooling rate was effective in reducing the density of defect states. This method will be useful for curing minority carrier annihilation defects generated in semiconductor device fabrication.

4. Conclusions

We reported a simple annealing method using a commercial 2.45 GHz microwave oven at 700 W to increase τ_{eff} for 4-in.-size 500-μm-thick 20 Ω cm n-type silicon substrates coated with 100-nm-thick thermally grown SiO_2 layers. The microwave annealing was conducted with 2-mm-thick glass substrates, which sandwiched the silicon samples to maintain the thermal energy and realize gradual cooling. We used a 9.35 GHz microwave transmittance measurement system to precisely measure τ_{eff} in the cases of CW 635 and 980 nm LD light illumination. An X–Y moving stage allowed measurement of the τ_{eff} spatial distribution of samples. Experimental τ_{eff} values with the two-different wavelength light illuminations were analyzed by numerical calculation with a finite-element program including models of photo-induced carrier generation, and their diffusion and annihilation with τ_b, S_{top}, and S_{rear}. High τ_{eff} values in the range from 1.6×10^{-3} to 3.1×10^{-3} s between 635 and 980 nm LD light illuminations were observed for the initial samples. This means that the silicon surfaces were well passivated by the thermally grown SiO_2 layers and the silicon sample had a high crystalline quality with a high τ_b. Ar plasma irradiation at 50 W for 60 s markedly decreased τ_{eff} to values in the range from 6.0×10^{-6} to 2.4×10^{-5} s in the case of 635 nm

© 2013 The Japan Society of Applied Physics

light illumination and from 4.2×10^{-5} to 6.4×10^{-5} s in the case of 980 nm light illumination. Numerical analysis revealed that high densities of recombination defect states localized at the silicon top surface in the range from 1.3×10^{13} to 5.0×10^{13} cm^{-2} caused far different experimental τ_{eff} values between the 635 and 980 nm CW light illuminations. Microwave annealing at 700 W for 120 s increased τ_{eff} to values in the range from 8.0×10^{-4} to 2.5×10^{-3} s, which are close to the values of the initial samples. The density of recombination defect states caused by Ar plasma irradiation was greatly decreased by microwave annealing to low values in the range from 7.0×10^{10} to 3.4×10^{11} cm^{-2}. The high τ_{eff} obtained by microwave annealing was maintained for a long time, above 5000 h.

Acknowledgement

This work was partly supported by Grant-in-Aid for Scientific Research C (Nos. 22560292 and 23560360) from the Ministry of Education, Culture, Sports, Science and Technology of Japan.

1) S. M. Sze: *Semiconductor Devices* (Wiley, New York, 1985) Chap. 7.
2) G. S. Kousik, Z. G. Ling, and P. K. Ajmera: J. Appl. Phys. **72** (1992) 141.
3) J. M. Borrego, R. J. Gutmann, N. Jensen, and O. Paz: Solid-State Electron. **30** (1987) 195.
4) G. W. 't Hooft, C. Van Opdorp, H. Veenvliet, and A. T. Vink: J. Cryst. Growth **55** (1981) 173.
5) H. Daio and F. Shimura: Jpn. J. Appl. Phys. **32** (1993) L1792.
6) J. Sritharathikhun, C. Banerjee, M. Otsubo, T. Sugiura, H. Yamamoto, T. Satoi, A. Limmanee, A. Yamada, and M. Konagai: Jpn. J. Appl. Phys. **46** (2007) 3296.
7) Y. Takahashi, J. Nigo, A. Ogane, Y. Uraoka, and T. Fuyuki: Jpn. J. Appl. Phys. **47** (2008) 5320.
8) M. Boulou and D. Bois: J. Appl. Phys. **48** (1977) 4713.
9) Y. Ogita: J. Appl. Phys. **79** (1996) 6954.
10) C. Munakata: Jpn. J. Appl. Phys. **43** (2004) L1394.
11) J. W. Corbett, J. L. Lindestrom, S. J. Pearton, and A. J. Tavendale: Sol. Cells **24** (1988) 127.
12) B. L. Sopori: Sol. Energy Mater. Sol. Cells **41–42** (1996) 159.
13) I.-W. Wu, A. G. Lewis, T.-Y. Hung, and A. Chiang: IEEE Electron Device Lett. **10** (1989) 123.
14) T. Sameshima and M. Satoh: Jpn. J. Appl. Phys. **36** (1997) L687.
15) K. Sakamoto and T. Sameshima: Jpn. J. Appl. Phys. **39** (2000) 2492.
16) M. Hasumi, J. Takenezawa, T. Nagao, and T. Sameshima: Jpn. J. Appl. Phys. **50** (2011) 03CA03.
17) T. Sameshima, K. Betsuin, T. Nagao, and M. Hasumi: Proc. Workshop Active Matrix Flat Panel Displays, 2012, 4-2.
18) T. Sameshima, H. Hayasaka, and T. Haba: Jpn. J. Appl. Phys. **48** (2009) 021204.
19) T. Sameshima, T. Nagao, S. Yoshidomi, K. Kogure, and M. Hasumi: Jpn. J. Appl. Phys. **50** (2011) 03CA02.
20) T. Sameshima, Y. Takiguchi, T. Nagao, and M. Hasumi: Proc. Workshop Active Matrix Flat Panel Displays, 2012, p. 43.
21) E. D. Palk: *Handbook of Optical Constants of Solids* (Academic Press, London, 1985) p. 547.
22) A. S. Groove: *Physics and Technology of Semiconductor Devices* (Wiley, New York, 1967) Chap. 5.
23) A. Goldsmith, T. E. Waterman, and H. J. Hirschorn: *Handbook of Thermophysical Properties of Solid Materials* (Pergamon Press, New York, 1961) Vols. 1 and 3.
24) K. Winer: Phys. Rev. B **41** (1990) 12150.
25) D. J. Fitzgerald and A. S. Grove: Proc. IEEE **54** (1966) 1601.

© 2013 The Japan Society of Applied Physics